VersionFinal, 12/07/2011

Minimization of spectral pattern changes during HRMAS experiments at 37 celsius degrees by prior focused microwave irradiation.

Davila M[1,2], Candiota AP[2,1], Pumarola M[3], Arus C[1,2,4]

[1] Departament de Bioquímica i Biologia Molecular, Unitat de Bioquímica de Biociències, Edifici Cs, Universitat Autònoma de Barcelona, 08193 Cerdanyola del Vallès, Spain

[2] Centro de Investigación Biomédica en Red en Bioingeniería, Biomateriales y Nanomedicina (CIBER-BBN), Spain

[3] Murine Pathology Unit, Centre de Biotecnologia Animal i Teràpia Gènica (CBATEG), Universitat Autònoma de Barcelona, 08193 Cerdanyola del Vallès, Spain

[4] Institut de Biotecnologia i de Biomedicina, Universitat Autònoma de Barcelona, 08193 Cerdanyola del Vallès, Spain

Corresponding author: Carles Arús

phone: +34 93 581 1257 fax +34 93 581 1264

email: carles.arus@uab.es

Abstract (max 200 words: presently 200 words)

Object

High-Resolution Magic Angle Spinning (HRMAS) magnetic resonance spectroscopy provides detailed metabolomic information from intact tissue. However, long acquisition times and high rotation speed may lead to time-dependent spectral pattern changes, which may affect proper interpretation of results. We report a strategy to minimize those changes, even at physiological recording temperature.

Materials and methods

Glioblastoma (Gbm) tumours were induced in 6 mice by stereotactic injection of GL261 cells. Animals were sacrificed and tumours were removed, halved and stored in liquid N_2. One aliquot from each sample was exposed to focused microwave (FMW) irradiation prior to HRMAS while the other half was not. Time-course experiments (374 min at 37^{o}C, 9.4T, 3000 Hz spinning rate) were carried out to monitor spectral pattern changes. Differences were assessed with Unianova test while post-HRMAS histopathology analysis was performed to assess tissue integrity.

Results

Significant changes (up to 2-fold) were observed in samples without FMW irradiation in several spectral regions e.g. mobile lipids/lactate (0.90-1.30ppm), acetate (1.90ppm), N-acetyl aspartate (2.00ppm), and Choline-containing compounds (3.19-3.25ppm). No significant changes in the spectral pattern of FMW-irradiated samples were recorded.

Conclusion

We describe here a successful strategy to minimize spectral pattern changes in mouse Gbm samples using a FMW irradiation system.

Keywords

Biopsy – Glioma – Metabolomics – NMR

Abbreviation List

Ac – Acetate

Ala - Alanine

Asp - Aspartate

Cho – Choline

ChCCp – Choline-containing compounds

Gly – Glycine

Glu - Glutamine

GPCho – Glycerophosphocholine

FMW – Focused Microwave

HRMAS - High-resolution magic angle spinning

ML – Mobile Lipids

MRS – Magnetic Resonance Spectroscopy

NAA – N-Acetyl Aspartate

Lac – Lactate

PCho – Phosphocholine

PtdCho – Phosphatidylcholine

Introduction

Ex vivo High-Resolution Magic Angle Spinning (HRMAS) proton (^{1}H) Nuclear Magnetic Resonance (NMR) spectroscopy has become an extremely versatile tool to study heterogeneous biological systems [1-11], being increasingly used to examine tissue biochemistry in a non-destructive way. HRMAS allows high-resolution spectra to be obtained directly from biopsy tissue and to determine and even quantify, its metabolome without losing information from lipids and macromolecules, which may be lost upon prior extraction. One of the relevant applications of HRMAS is the analysis of the metabolic profile of human brain tumour samples [2,8,9,10,12,13-16]. In this sense, the ability of evaluating the whole sample metabolome contributes to correlate better *in vivo* and *ex vivo* spectra of human brain tumours [17-19] and gives important information to improve the potential of *in vivo* ^{1}H NMR spectroscopy as a noninvasive diagnostic tool.

However, the biochemical profile obtained by HRMAS may be affected by experimental factors such as the period of ischemia before snap-freezing of the biopsy tissue for subsequent analysis, the mechanical stress of the spinning procedure of HRMAS itself [8,10], the storage of the sample [20-22], and the temperature of acquisition [20-22]. To minimize biochemical changes during the NMR acquisition time, most HRMAS studies are performed at about 2-4^o C, with samples initially kept in sub-zero storage before HRMAS acquisition, but biological processes, e.g. enzymatic reactions, do not stop even at temperatures close to 0^o C. In addition, long acquisition times may be required if 2D experiments have to be carried out during the study [23,24,11]. On the other hand, higher and more physiologic temperatures seem to allow better detection of resonances from mobile lipids (ML) and Choline-containing compounds (ChCCp) [16]. This can be of interest because it has been shown that these resonances may act as cell proliferation markers in cellular models [25-27], as well as in brain tumour tissue [28] and cervical tumours [29]. These metabolites have also proven to be relevant in pattern recognition studies using the HRMAS spectral vectors as in[24]. Then, on one hand, we may want to record HRMAS at 37^{o}C and for long periods of time to improve

information content of the recorded pattern while, on the other hand, it is important that the spectral features observed are reliable avoiding excessive change due to postmortem metabolism, which may increase unwanted "noise" possibly blurring initial HRMAS pattern differences.

There have been few studies specifically designed to assess the biochemical changes, that may occur as a result of different sample-handling strategies and experimental delays (as in [20,8,10]). In our case, we propose a new sample preservation strategy to reduce changes in spectral patterns of tissue biopsies due to experimental factors during data acquisition. A study with murine glioma samples has been designed in order to investigate that.

Focused microwave irradiation (FMW) is a widely used method to arrest metabolic processes and, consequently, preserve the metabolome of samples or tissues. The use of this method which rapidly heats the brain to 82-85^{o}C in milliseconds, causing the inactivation of enzyme activity, has been previously described by other authors [30-38] . For example, authors in [35] indicated that the FMW rapidly inactivate enzymes and prevents post mortem breakdown of adenine nucleotides and adenosine, thereby enabling accurate measurements of AMP, ADP, ATP and adenosine [33] and glycogen [37] from rat brain. Additionally, authors in [38] demonstrated that FMW did allow HRMAS analysis of rat brain tissue after sacrifice and quantification of ^{13}C enrichment in selected metabolites with resolution comparable to the hydrosoluble extract data. Finally, FMW has also been used as a sacrifice method to quantify glucose content in GL261 tumours after HRMAS analysis of dissected tumour or peritumoral sections of mice brain [36]. The previously mentioned authors have used the FMW irradiation to euthanize animals and to preserve the metabolomic pattern of the in vivo animal brain or brain tumour. This is a good approach for preclinical brain tumour models, but for obvious reasons it is not feasible for human brain tumours. In this sense, we have designed an intermediate approach, which takes into account the usual conditions of human brain biopsies collection and storage. We hypothesized that performing the FMW irradiation while the biopsy is still frozen and prior to proceeding with the HRMAS acquisition, should preserve the sample

metabolome and avoid further changes due to long acquisition times at physiological temperatures or due to high spinning rates.

Additionally, in order to evaluate possible tissue integrity changes, some samples have been analyzed by post-HRMAS histopathology.

Materials and methods

Animals and cells

A total of 6 C57BL/6 mice were used in this study. These were obtained from Charles River Laboratories (France) and housed at the animal facility of our institution (Servei d'Estabulari, Universitat Autònoma de Barcelona). All animal studies were approved by the local ethics committee, according to the regional and state legislation (protocol DARP-4600/CEEAH-530). GL261 mouse glioma cells were obtained from the Tumor Bank Repository at the National Cancer Institute (Frederick/MD, USA) and were grown as described in [39].

Brain Tumours

Tumours were induced in mice by intracranial stereotactic injection of 10^5 GL261 cells in the caudate nucleus, essentially as described previously [39].

Tissue sample collection and preparation

Tumour-bearing animals were sacrificed with an intraperitoneal injection of pentobarbital (50mg/kg, 60mg/ml). The tumour was removed and frozen in liquid N_2 immediately (5 ±1min). Tumour samples (n=3) were split into two visually equal parts, setting two sample groups (with FMW and without FMW, N-FMW) with n=3 in each one, and stored in liquid N_2 until further analysis.

FMW Irradiation of tissue samples

Each sample of the FMW irradiation group (n=3) was allowed to increase in temperature in a Petri dish, while the temperature of the sample was controlled with a temperature probe (TES Electrical Electronic Corp). When the sample temperature reached 0^oC, it was placed inside a cryogenic tube in a mouse accessory for FMW irradiation (Water-Jacketed mouse

holder, Muromachi, Kikai Co., LTD.) and it was FMW-irradiated (5kW during 2.6s, due to the low temperature of the sample). The cryogenic tube should not be capped too tightly to allow for a possible water vapor generated to escape. It is very important to ensure that the sample is in the exact position required (placed at the bottom of the cryogenic tube), because the focused microwave is directed and optimized for the animal size (mouse or rat) accessory in order to concentrate in the animal brain. After irradiation, the sample was recovered with spatula and transferred to the HRMAS rotor as described in the HRMAS ^{1}H Spectroscopy section.

HRMAS ^{1}H Spectroscopy

Rotor Preparation: Frozen tumour tissue samples (11.28 ± 5.3mg) either irradiated (group FMW) or non irradiated (group N-FMW), were split in small pieces to fit into the zirconium rotor with a 50 µl cylindrical insert (Cortecnet, France). Pre-cooled D_2O-saline (0.15 M NaCl) was added (10.0±5.0 µl) into the rotor to allow for the lock signal detection.

The HRMAS experiments were carried out in a Bruker Advance III spectrometer operating at 9.4T (400MHz for ^{1}H) (*Servei de Ressonància Magnètica Nuclear- Universitat Autònoma de Barcelona*) using the pulse-and-acquire sequence with water presaturation during 2s at 0.042mW. The sweep width was 10ppm (4000Hz), and 16k points (8k real) were acquired. The number of transients was 512 (34min) and acquisition time was 2.04s (total recycling time: 4.04s) and the spinning rate was 3000Hz.

Time-course experiments (374 min total time, 6.2h) were performed to monitor the spectral pattern changes. A total of 11 spectra were acquired at 37^{o} C actual rotor temperature while spinning at 3000 Hz, simulating the physiological temperature conditions. An additional time-course experiment was carried out (34 min total time) to investigate possible changes taking place during the initial 34 minutes period. Spectra were recorded every 2 minutes, with the same acquisition parameters as described before, except that the number of transients was 2. In both time course experiments, the temperature calibration was previously carried out using a rotor filled with ethylenglycol as described in [40].

Data processing

Spectra were processed with TopSpin 1.3 (Bruker Daltonik, Gmbh). Prior to Fourier transform, 0.5Hz line broadening was applied. The chemical shift calibration was carried out setting the total creatine singlet at 3.03 ppm, the spectra were phased and the vertical baseline offset corrected.

The normalization of the spectral data vectors in ASCII format was carried out using home-made scripts in the R statistical programming language [41]. The unit-length normalization was applied for the region between 0.5 - 4.5 ppm of each spectrum according to equation 1 as in [16] and the peak intensities at selected frequencies (X) were used as input for further statistical analyses. The initial intensity of the resonances of interest was set to 100% and the variation was calculated as a fraction of the initial intensity.

$$\frac{X^2}{\sqrt{\sum_{i=1}^{i=n} X_n^2}} = \text{Normalized intensity} \qquad \text{Eq. [1]}$$

Statistical analysis

The Unianova test was performed using the statistics toolbox of SPSS for Windows software, version 17 (SPSS, Chicago, IL, USA) to evaluate the existence of statistically significant differences. A General Lineal Model (GLM) was applied in order to determine whether certain chosen signal normalized intensity was globally different along time-course experiments in FMW and N-FMW samples. The significance level was set at $p<0.05$.

Post HRMAS histopathology

After HRMAS analysis, all tissue samples were fixed in 4% buffered formaldehyde during 6-24h, and fixed samples were routinely included in paraffin; slices of 4µm were obtained from each sample and were stained with haematoxylin-eosin. These samples were evaluated by a

neuropathologist from (MP) the Murine Pathology Unit of the CBATEG (*Centre de Biotecnologia Animal i Teràpia Gènica, Universitat Autònoma de Barcelona*).

Results

Typical pattern and tentative assignments of major resonances

A typical HRMAS spectrum of the high field part of one GL261 mouse glioma tissue sample is shown in Fig. 1. Tentative assignments were carried out according to [11,42]. As expected from previous work [36,39], GL261 Gbm tumour tissue, even after short post mortem ischemia, shows high lactate (Lac) and alanine (Ala) content, and also high choline-containing compounds (ChCCp), whereas N-acetyl aspartate (NAA) is very low.

HRMAS spectral pattern changes during incubation time at 37^{o}C

Significant changes were detected in the spectral pattern of samples without FMW irradiation with increasing incubation time, while FMW irradiated samples showed no visually detectable change in the HRMAS spectral pattern (Figures 2 and 3). The most significant changes in normalized intensity of resonances (table 1) takes place in the 3.19 ppm resonance (the trymethylamine group of free choline (Cho)) that increases 2-fold in time course experiments and in the 3.21 ppm resonance of phosphocholine (PCho) which increases by 45%. No equivalent increase seems to take place in glycerophosphocholine (GPCho) at 3.23 ppm, which in fact decreases down to 80% of its initial value. Visually (figure 2, bottom), the Ptdcho + glycerophosphocholine (GPCho) variation does not seem to account for the Cho + PCho increase. Accordingly, this would suggest that the increase in free Cho and PCho originates from the postmortem activity of phospholipases and phosphatases [43,44] acting on phospholipids at cellular membranes of an HRMAS-invisible ChCCp pool. This pool cannot be the already HRMAS visible PtdCho pool originating the resonance at 3.25 ppm, which does not decrease in apparent intensity. In addition, the representative GL261 sample spectra (figure 2) show significant differences in acetate (Ac) intensity at 1.90 ppm, which shows 2-fold increase. The concomitant reduction of the NAA (table 1) suggests that the increase in Ac and visible Asp

(at about 2.62–2.82 ppm) should at least be partially linked to the NAA degradation. On the other hand, surprisingly, no significant changes were detected in the Lac region, demonstrating that the high intensity of the Lac resonance is caused by the ischemia time post-sacrifice (about 5min) and prior to freezing the sample in liquid nitrogen, or already present in the in vivo tumour. These results agree with previous data from our group on HRMAS and MRS of GL261 tumours [36,39], which used a FMW sacrifice method prior to HRMAS analysis and for which an in vivo Lac content of 7.9 ± 1.8 μmol/g water was detected in the investigated mice. A further aspect to consider is the intrinsic variability of the GL261 tumour pattern, as can be seen in figure 2, the initial intensity for Lac, ML or ChCCp was clearly different for different tumour aliquots. This heterogeneity of GL261 tumours has already been described [39].

The statistical evaluation of time course curves, carried out with the Unianova method, shows that normalized intensities of selected signals (Ac, ChCCp) presented a significantly ($p = <0.001$) different behavior between FMW and N-FMW irradiated samples. The results obtained with the comparison between samples from different groups along the acquisition time are shown in table 1. On the other hand, changes showed tendency for significance for ML (1.30ppm) and NAA. No significant changes were detected in the downfield region of the spectrum (results not shown).

Post HRMAS histopathology

Tissue samples after FMW irradiation plus 374min of HRMAS analysis (FMW group) and after HRMAS analysis alone (N-FMW group) were analyzed by histopathological techniques. The referring pathologist (MP) was asked to evaluate the presence/absence of tumour cells, their overall morphology and if a tumour diagnosis would be confirmed even with possible changes caused by FMW irradiation or spinning rates. All evaluated (n=6) samples could be perfectly recognized as high grade glial tumour (fig.4), although some artifactual morphology and pyknotic nuclei were detected in some samples, maybe due to both FMW irradiation and high spinning rates [12,45].

Discussion

Most recent HRMAS work was performed at 0^{o} – 4^{o} C and using short total acquisition times to reduce the risk of tissue degradation. Furthermore, freezing and thawing cycles are likely to cause unpredictable amounts of cell damage and lysis [22]. On the other hand, the use of higher physiological temperature has been proved to help in a better detection of macromolecules, ML and ChCCp signals in brain tissue samples [1, 16].

The present study shows that the use of FMW irradiation in frozen biopsy/tumour samples is able to stabilize the HRMAS spectral pattern and avoid changes due to further post-mortem metabolism, even when acquiring spectra at normal body temperature. The main early spectral pattern changes observed in tissue samples are usually related to anaerobic glycolysis activation, for example, a marked increase of lactate [46,47].

Among the main spectral pattern changes detected in this study, there is an increase of about 2-fold of the Ac signal at 1.90ppm in non-FMW irradiated samples along the 374min time course, whereas in FMW irradiated samples no significant changes were detected. In this sense, authors in [1] performed HRMAS studies on the degradation of human and monkey brain at 20^{o}C and their results pointed that the increase in Ac was mostly due to the degradation of NAA, although Ac may also be produced by other neurochemical degradation processes. The changes in the spectral pattern observed by these authors were markedly reduced when the experimental temperature was changed from 20°C to 2°C which is also in agreement with results reported by authors in [8]. Moreover, considering the individual values obtained at the start and at the end of our experiments, the decrease in the NAA signal is qualitatively equivalent to the increase in the Ac signal, which seems to agree with the production of Ac being closely related in our case with the NAA degradation. A decrease of NAA with time in halothane-euthanized rats was also described in [47], and this decrease was prevented by prior FMW sacrifice of the animal.

The changes observed in ChCCp signals are in full agreement with results reported by authors in [8]. A marked increase was observed for Cho and PCho signals in their work (around

1.5 fold between 0 and 0.5h) which remained essentially unchanged along the 4h time period studied at 4^{o} C, in qualitative agreement with results presented in our work. Regarding to the GPCho signal, we have detected a decrease in this compound along the acquisition time in N-FMW irradiated samples. In FMW-irradiated samples, the Cho signal shows minor non-significant increases, around 11%, while PCho and PtdCho signals remain essentially unchanged. We should take into account that the spinning rate used in our experiments, in addition to the long acquisition time, could increase the observability of the ChCCp possibly through the action of phospholipases and other enzymes upon biological membranes. These plasma membrane phospholipids would constitute an NMR invisible pool even at the HRMAS conditions used here, and be different then from the HRMAS-visible PtdCho pool that does barely change when free Cho and PCho increase in N-FMW biopsies.

In this study we mainly focused on analyzing spectral features that had been reported to change along the acquisition time when acquiring spectra at physiological temperatures [16]. Nevertheless, we have also evaluated whether other significant changes may occur for example due to freezing and thawing samples with and without FMW irradiation, e.g. in the content of Ala, Glu and Gly [48,12]. Authors in [12] have also suggested that Gly could be at a higher 'NMR visible' concentration when analyzing a sample with HRMAS techniques and the source of this "extra" Gly could be due either to the post-mortem metabolism or to the release of a 'bound' species because of the sample damage that can occur in the HRMAS experiment, resulting from the time required to acquire quantitative 1D spectra with long HRMAS protocols (2.5hr). In our case we should rule out the storage time as the source of changes in the Gly pattern, because no difference was detected among FMW and non-FMW treated samples.

The stabilization of the spectral pattern achieved with this method could have relevance for pattern recognition studies [16,24]. Authors in [24] have performed pattern recognition using HRMAS spectral features to distinguish tumour/tissue types (normal, high-grade tumours, low-grade tumours) and subtypes (glioblastoma, anaplastic astrocytoma,

meningioma, schwannoma, pylocytic astrocytoma and metastasis) and some of the selected features relevant to their tumour discrimination overlap with features studied in our work (ML, NAA, ChCCp).

Regarding histopathological analysis, previous studies have shown that samples could be analyzed by histopathology after HRMAS studies [45,12,16]. Authors in [45] pointed that this post-HRMAS analysis of GBM samples sometimes shows a non-negligible lack of characteristic malignant and necrotic histopathological features, so maybe regions of necrosis could be compressed by the high sample spinning rate. We did not observe such a morphological change in our study, and further investigation is needed in order to determine whether FMW irradiation would be even useful for preserving the architecture of the tissue, in addition to avoiding spectral pattern changes due to post-mortem metabolism.

In summary, the postmortem metabolic changes observed in our N-FMW biopsy samples are in agreement with results reported by other authors, being expected when working at physiological temperatures and long acquisition times. On the other hand, the lack of significant changes in the HRMAS pattern achieved in FMW samples should be advantageous for reducing the “noise” introduced by post-mortem metabolism in the recorded spectra. This may facilitate future metabolomic work in biopsies, especially when requiring long acquisition times, both for preclinical and for human brain tumour biopsies.

Conclusions

We have developed an experimental strategy to preserve the HRMAS spectral pattern of frozen tissue biopsies using prior FMW irradiation. No significant spectral pattern changes have been observed even after 374 min of acquisition at 37^{o}C, in comparison with N-FMW samples. This method will be useful to ensure that sample pattern will remain stable in long HRMAS data acquisitions (e.g. 2D experiments). Besides, the histopathology analysis of the investigated samples may still be performed after FMW irradiation and HRMAS acquisition.

This metabolome fixation method could be applied in the future to human brain tumour biopsies collected to carry out metabolomic and pattern recognition analysis of data.

Acknowledgements

We thank *Universitat Autonòma de Barcelona* (Spain) for the pre-doctoral fellowship to Myriam Dávila. We also thank Milena Acosta and Teresa Delgado-Goñi for their help with preclinical tumour model generation. Work was funded by PHENOIMA (MICINN SAF 2008-0332). This work was also partially funded by the *Centro de Investigación Biomédica en Red – Bioingeniería, Biomateriales y Nanomedicina* which is an initiative of the *Instituto de Salud Carlos III (Spain)* co-funded by EU FEDER funds.

References

1. Cheng L, Ma M, Becerra L, Ptak T, Tracey I, Lackner A, González R (1997) Quantitative neuropathology by high resolution magic angle spinning proton magnetic resonance spectroscopy. Proc Natl Acad Sci U S A 94 (12):6408-6413
2. Cheng LL, Chang IW, Louis DN, Gonzalez RG (1998) Correlation of high-resolution magic angle spinning proton magnetic resonance spectroscopy with histopathology of intact human brain tumor specimens. Cancer Res 58 (9):1825-1832
3. Morvan D, Demiden A, Papon J, Madelmont JC (2003) Quantitative HRMAS proton total correlation spectroscopy applied to cultured melanoma cells treated by chloroethyl nitrosourea: demonstration of phospholipid metabolism alterations. Magn Reson Med 49:241-248
4. Griffin JL, Bollard M, Nicholson JK, Bhakoo K (2002) Spectral profiles of cultured neuronal and glial cells derived from HRMAS 1H NMR spectroscopy. NMR Biomed 15:375-384
5. Valonen PK, Griffin JL, Lehtimäki KK, Liimatainen T, Nicholson JK, Gröhn OHJ, Kauppinen RA (2005) High-resolution magic-angle-spinning 1H NMR spectroscopy reveals different responses in choline-containing metabolites upon gene therapy-induced programmed cell death in rat brain glioma. NMR Biomed 18:252-259
6. Ratai EM, Pilkenton S, Lentz MR, Greco JB, Fuller RA, Kim JP, He J, Cheng LL, Gonzalez G (2005) Comparisons of brain metabolites observed by HRMAS 1H NMR of intact tissue and solution 1H NMR of tissue extracts in SIV-infected macaques. NMR Biomed 18:242-251
7. Yang Y, Li C, Nie X, Feng X, Chen W, Yue Y, Tang H, Deng F (2007) Metabonomic studies of human hepatocellular carcinoma using high-resolution magic-angle spinning 1H NMR spectroscopy in conjunction with multivariate data analysis. J Proteome Res 6 (7):2605-2614
8. Opstad KS, Bell BA, Griffiths JR, Howe FA (2008) An assessment of the effects of sample ischaemia and spinning time on the metabolic profile of brain tumour biopsy specimens as determined by high-resolution magic angle spinning (1)H NMR. NMR Biomed 21 (10):1138-1147
9. Righi V, Andronesi O, Mintzopoulos D, Black P, Tzika A (2010) High-resolution magic angle spinning magnetic resonance spectroscopy detects glycine as a biomarker in brain tumors. Int J Oncol 36 (2):301-306

10. Martinez-Bisbal MC, Esteve V, Martinez-Granados B, Celda B (2011) Magnetic resonance microscopy contribution to interpret high-resolution magic angle spinning metabolomic data of human tumor tissue. J Biomed Botechnol 2011
11. Martinez-Bisbal MC, Marti-Bonmati L, Piquer J, Revert A, Ferrer P, Llacer JL, Piotto M, Assemat O, Celda B (2004) 1H and 13C HR-MAS spectroscopy of intact biopsy samples ex vivo and in vivo 1H MRS study of human high grade gliomas. NMR Biomed 17 (4):191-205
12. Wright A, Fellows G, Griffiths J, Wilson M, Bell B, Howe F (2010) Ex-vivo HRMAS of adult brain tumours: metabolite quantification and assignment of tumour biomarkers. Mol Cancer 9:66
13. Monleón D, Morales J, Gonzalez-Darder J, Talamantes F, Cortés O, Gil-Benso R, López-Ginés C, Cerdá-Nicolás M, Celda B (2008) Benign and atypical meningioma metabolic signatures by high-resolution magic-angle spinning molecular profiling. J Proteome Res 7 (7):2882-2888
14. Poullet JB, Martinez-Bisbal MC, Valverde D, Monleon D, Celda B, Arus C, Van Huffel S (2007) Quantification and classification of high-resolution magic angle spinning data for brain tumor diagnosis. Conf Proc IEEE Eng Med Biol Soc 2007:5407-5410
15. Opstad KS, Bell BA, Griffiths JR, Howe FA (2008) Toward accurate quantification of metabolites, lipids, and macromolecules in HRMAS spectra of human brain tumor biopsies using LCModel. Magn Reson Med 60 (5):1237-1242
16. Valverde-Saubí D, Candiota AP, Molins MA, Feliz M, Godino O, Davila M, Acebes JJ, Arus C (2010) Short-term temperature effect on the HRMAS spectra of human brain tumor biopsies and their pattern recognition analysis. MAGMA 23 (4):203-215
17. Opstad KS, Wright AJ, Bell BA, Griffiths JR, Howe FA (2010) Correlations between in vivo (1)H MRS and ex vivo (1)H HRMAS metabolite measurements in adult human gliomas. J Magn Reson Imaging 31 (2):289-297
18. Davies N, Wilson M, Natarajan K, Sun Y, MacPherson L, Brundler M, Arvanitis T, Grundy R, Peet A (2010) Non-invasive detection of glycine as a biomarker of malignancy in childhood brain tumours using in-vivo 1H MRS at 1.5 tesla confirmed by ex-vivo high-resolution magic-angle spinning NMR. NMR Biomed 23 (1):80-87
19. Sjobakk TE, Johansen R, Bathen TF, Sonnewald U, Juul R, Torp SH, Lundgren S, Gribbestad IS (2008) Characterization of brain metastases using high-resolution magic angle spinning MRS. NMR Biomed 21 (2):175-185
20. Waters N, Garrod S, Farrant R, Haselden J, Connor S, Connelly J, Lindon J, Holmes E, Nicholson J (2000) High-resolution magic angle spinning (1)H NMR spectroscopy of intact liver and kidney: optimization of sample preparation procedures and biochemical stability of tissue during spectral acquisition. Anal Biochem 282 (1):16-23
21. Wu C, Taylor J, He W, Zepeda A, Halpern E, Bielecki A, RG G, LL. C (2003) Proton high-resolution magic angle spinning NMR analysis of fresh and previously frozen tissue of human prostate. Magn Reson Med 50 (6):1307-1311
22. Bourne R, Dzendrowskyj T, Mountford C (2003) Leakage of metabolites from tissue biopsies can result in large errors in quantitation by MRS. NMR Biomed 16:96-101
23. Erb G, Elbayed K, Piotto M, Raya J, Neuville A, Mohr M, Maitrot D, Kehrli P, Namer I (2008) Toward improved grading of malignancy in oligodendrogliomas using metabolomics. Magn Reson Med 59:959-965
24. Andronesi O, Blekas KD, Mintzopoulos D, Astrakas LG, Black PM, Tzika AA (2008) Molecular classification of brain tumor biopsies using solid-state magic angle spinning proton magnetic resonance spectroscopy and robust classifiers. Int J Oncol 33 (5):1017-1025
25. Barba I, Cabanas ME, Arus C (1999) The relationship between nuclear magnetic resonance-visible lipids, lipid droplets, and cell proliferation in cultured C6 cells. Cancer Res 59 (8):1861-1868
26. Quintero M, Cabanas ME, Arus C (2007) A possible cellular explanation for the NMR-visible mobile lipid (ML) changes in cultured C6 glioma cells with growth. Biochim Biophys Acta 1771 (1):31-44

27. Hakumäki JM, Kauppinen RA (2000) 1H NMR visible lipids in the life and death of cells. Trends Biochem Sci 25 (8):357-362
28. Barton SJ, Howe FA, Tomlins AM, Cudlip SA, Nicholson JK, Bell BA, Griffiths JR (1999) Comparison of in vivo 1H MRS of human brain tumours with 1H HR-MAS spectroscopy of intact biopsy samples in vitro. Magn Reson Mater Phy 8 (2):121-128
29. Mahon M, Williams A, Soutter W, Cox I, McIndoe G, Coutts G, Dina R, deSouza N (2004) 1H magnetic resonance spectroscopy of invasive cervical cancer: an in vivo study with ex vivo corroboration. NMR Biomed 17 (1):1-9
30. Passonneau JV, Lust WD, McCandless DW (1979) The preparation of biological samples for analysis of metabolites, vol B212. Elsevier / North Holland Scientific Publishers Ltd.
31. Sharf MT, Mackiewics M, Naidoo N, O'Callaghan JP, Pack AI (2008) AMP-activated protein kinase phosphorylation in brain is dependent on method of killing and tissue preparaton. J Neurochem 105:833-841
32. Kong J, Shepel PN, Holden CP, Mackiewicz M, Pack AI, J.D. G (2002) Brain Glycogen Decreases with Increased Periods of Wakefulness: Implications for Homeostatic Drive to Sleep. J neurosci 22 (13):5581-5587
33. Delaney SM, Giger JD (1996) Brain regional levels of adenosine and adenosine nucleotides in rats killed by high-energy focused microwave irradiation. J neurosci meth 64:151-156
34. Murphy EJ (2010) Brain fixation for analysis of barin lipid-mediators of signal transduction and brain eicosanoids requires head-focused microwave irradiation: an historical perspective. Prostaglandins Other Lipid Mediat 91:63-67
35. O'Callaghan JP, Sriram K (2004) Focused microwave irradiation of the brain preserves in vivo protein phosphorylation: comparison with other methods of sacrifice and analysis of multiple phosphoproteins. . J neurosci meth 135:159-168
36. Simoes RV, Delgado-Goni T, Lope-Piedrafita S, Arus C (2010) 1H-MRSI pattern perturbation in a mouse glioma: the effects of acute hyperglycemia and moderate hypothermia. NMR Biomed 23 (1):23-33
37. Lei H, Morgenthaler F, Yue T, Gruetter R (2007) Direct validation of in vivo localized 13C MRS measurements of brain glycogen. Magnetic Resonance in Medicine 57 (2):243-248
38. Risa Ø, Melø TM, Sonnewald U (2009) Quantification of amounts and 13C content of metabolites in brain tissue using high- resolution magic angle spinning 13C NMR spectroscopy. NMR in Biomedicine 22 (3):266-271
39. Simoes RV, Garcia-Martin ML, Cerdan S, Arus C (2008) Perturbation of mouse glioma MRS pattern by induced acute hyperglycemia. NMR Biomed 21 (3):251-264
40. Braun S, Kalinowski H-O, Berger S (1998) 150 and more basic NMR experiments. A practical course. WILEY-VCH Verlag GmbH, Weinheim
41. Ihaka RGaR (2011) R: A language and environment for statistical computing. 2.9 edn., WU, WIEN
42. Govindaraju V, Young K, Maudsley AA (2000) Proton NMR chemical shifts and coupling constants fro brain metabolites. NMR Biomed 13:129-153
43. Paris L, Cecchetti S, Spadaro F, Abalsamo L, Lugini L, Pisanu ME, Iorio E, Natali PG, Ramoni C, Podo F Inhibition of phosphatidylcholine-specific phospholipase C downregulates HER2 overexpression on plasma membrane of breast cancer cells. Breast Cancer Research 12 (3):R27
44. Roberts SJ, Stewart AJ, Sadler PJ, Farquharson C (2004) Human PHOSPHO1 exhibits high specific phosphoethanolamine and phosphocholine phosphatase activities. Biochem J 382 (1):59-65
45. Cheng LL, Anthony DC, Comite AR, Black PM, Tzika AA, Gonzalez RG (2000) Quantification of microheterogeneity in glioblastoma multiforme with ex vivo high-resolution magic angle spinning (HRMAS) prtoton magn. Neuro Oncol 2 (87-95)
46. Shank R, Aprison M (1971) Post mortem changes in the content and specific radioactivity of several aminoacids in four areas of the rat brain. J Neurobiol 2:145-115

47. De Graaf RA, Chowdhury GMI, Brown PB, Rothman DL, Behar KL (2009) In situ 3D magnetic resonance metabolic imaging of microwave-irradiated rodent brain: a new tool for metabolomics research. Journal of Neurochemistry 109 (2):494-501
48. Middleton DA, Bradley DP, Connor SC, Mullins PG, Reid DG (1998) The effect of sample freezing on proton magic-angle spinning NMR spectra of biological tissue. Magn Reson Med 40 (166-169)

Table

Chemical shift (ppm)	Fold change FMW	Fold change N-FMW	Metabolite	p-value
0.90	1.0±0.02	1.0±0.04	ML	0.556
1.30	1.0±0.04	1.0±0.01	ML	0.051
1.90	1.1±0.06	2.0±0.26	Ac	<0.001
2.02	0.8±0.24	0.5±0.07	NAA	0.061
2.62 – 2.82	1.1±0.12	1.4±0.11	Asp	0.303
3.19	1.1±0.10	2.1±0.15	Cho (choline)	<0.001
3.21	1.1±0.08	1.4±0.12	PCho (phosphocholine)	<0.001
3.23	1.0±0.01	0.8±0.02	GPCho (glycerophosphocholine)	0.035
3.25	1.0±0.01	1.1±0.08	PtdCho (phosphatidylcholine)	0.001

Table 1. Results from the Unianova test carried out to compare the significance for the variation along the time-course experiment for selected signal intensities from the HRMAS spectral pattern, comparing FMW and N-FMW time-course curves.

Figures

Figure 1

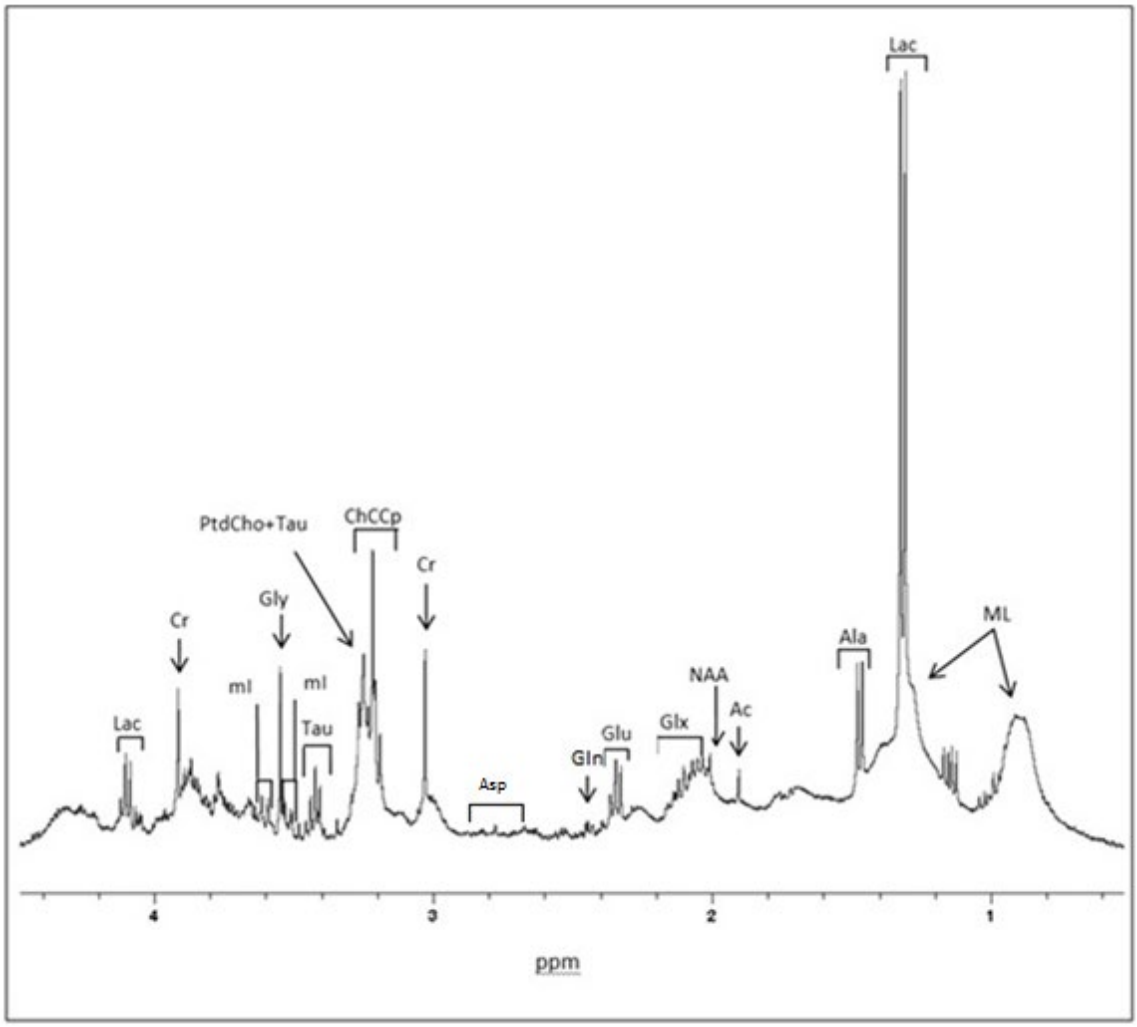

Figure 2

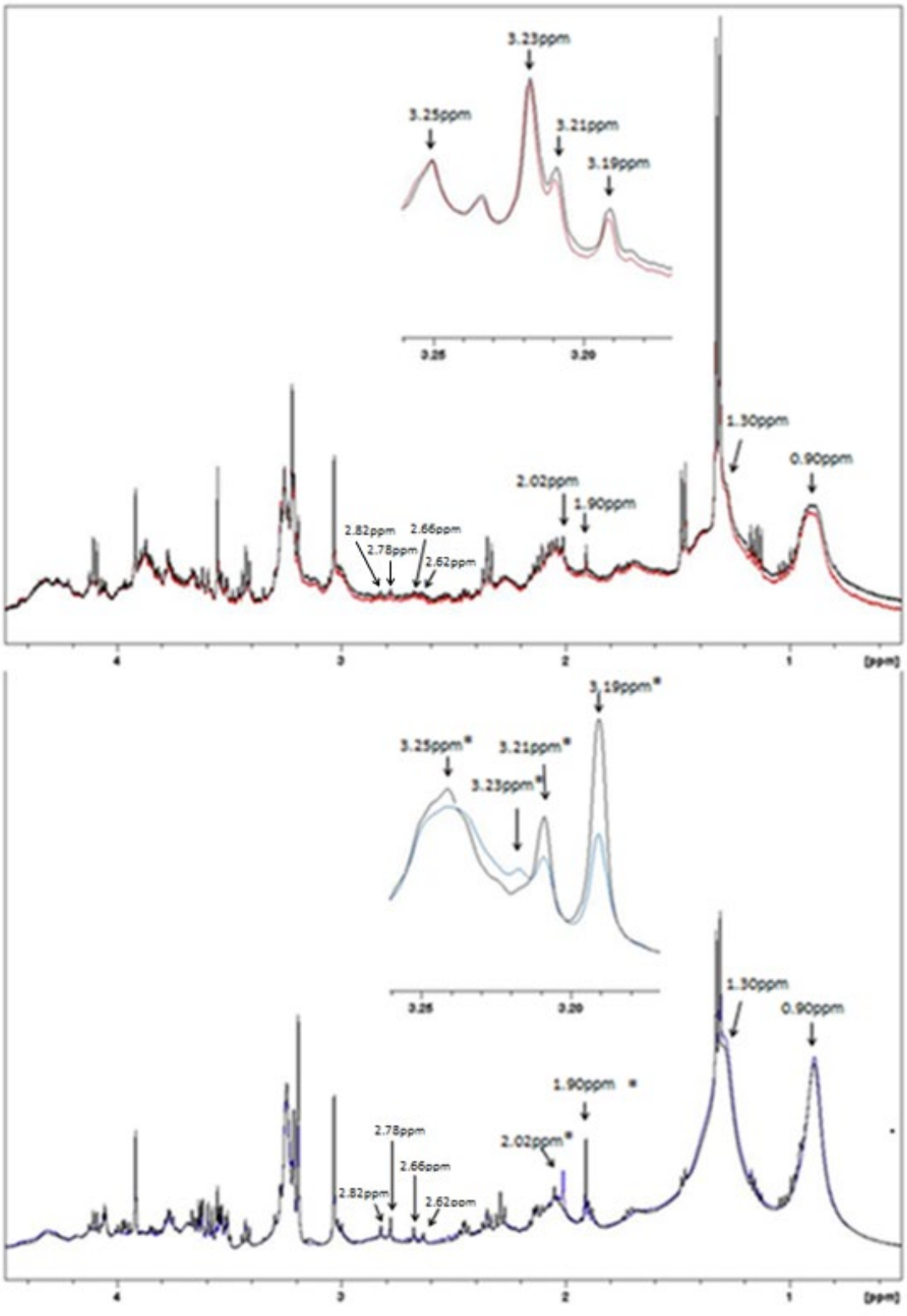
3.23ppm
3.25ppm
3.21ppm
3.19ppm
3.25
3.20
1.30ppm
0.90ppm
2.02ppm
1.90ppm
2.82ppm
2.66ppm
2.78ppm
2.62ppm
4
3
2
1
[ppm]
3.19ppm*
3.25ppm*
3.21ppm*
3.23ppm*
3.25
3.20
1.30ppm
0.90ppm
1.90ppm *
2.78ppm
2.02ppm*
2.66ppm
2.82ppm
2.62ppm
4
3
2
1
[ppm]

Figure 3

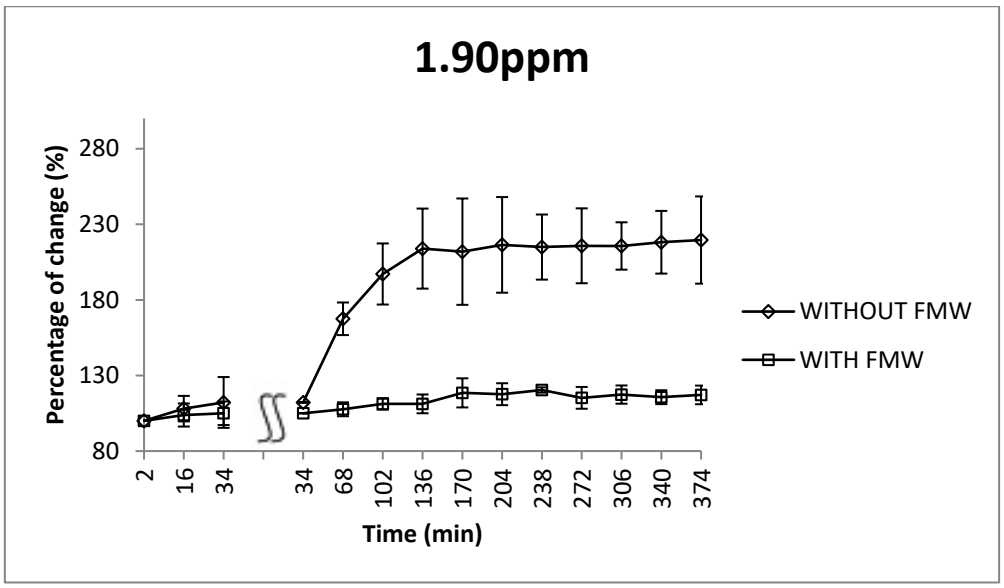
1.90ppm
Percentage of change (%)
280
230
180
130
80
2
16
34
34
68
102
136
170
204
238
272
306
340
374
Time (min)
WITHOUT FMW
WITH FMW

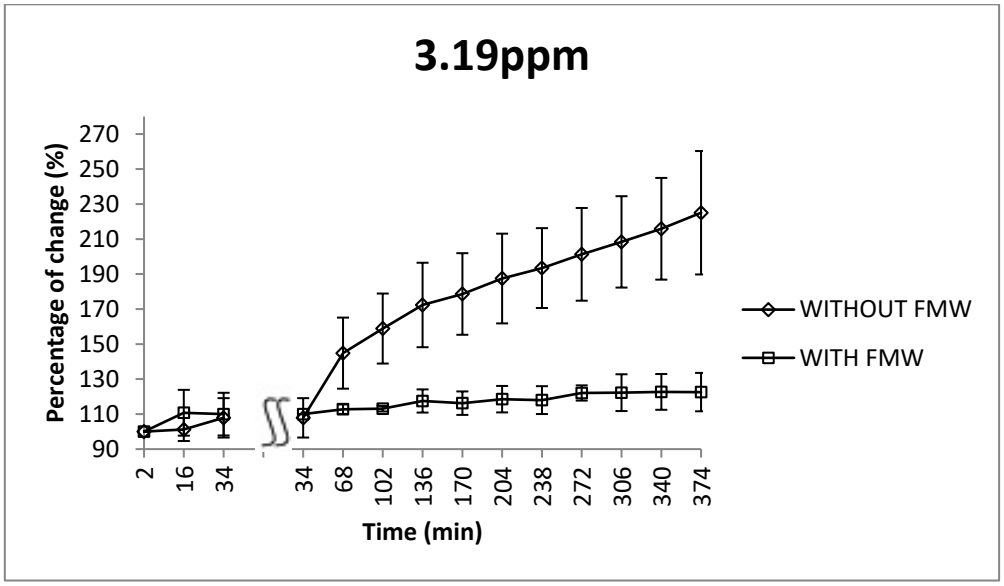
3.19ppm
Percentage of change (%)
270
250
230
210
190
170
150
130
110
90
2
16
34
34
68
102
136
170
204
238
272
306
340
374
Time (min)
WITHOUT FMW
WITH FMW

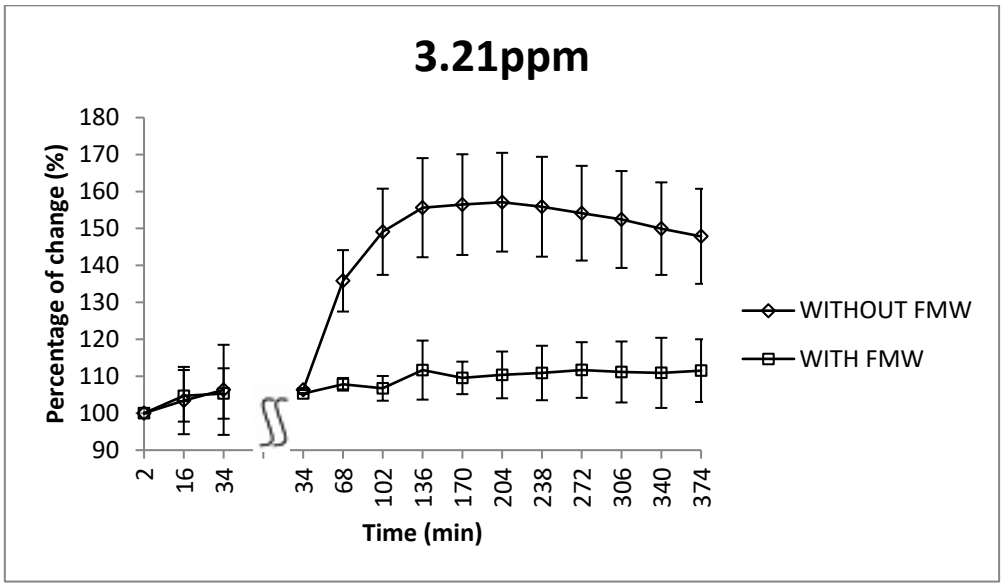
3.21ppm
Percentage of change (%)
180
170
160
150
140
130
120
110
100
90
2
16
34
34
68
102
136
170
204
238
272
306
340
374
Time (min)
WITHOUT FMW
WITH FMW

Figure 4

a)

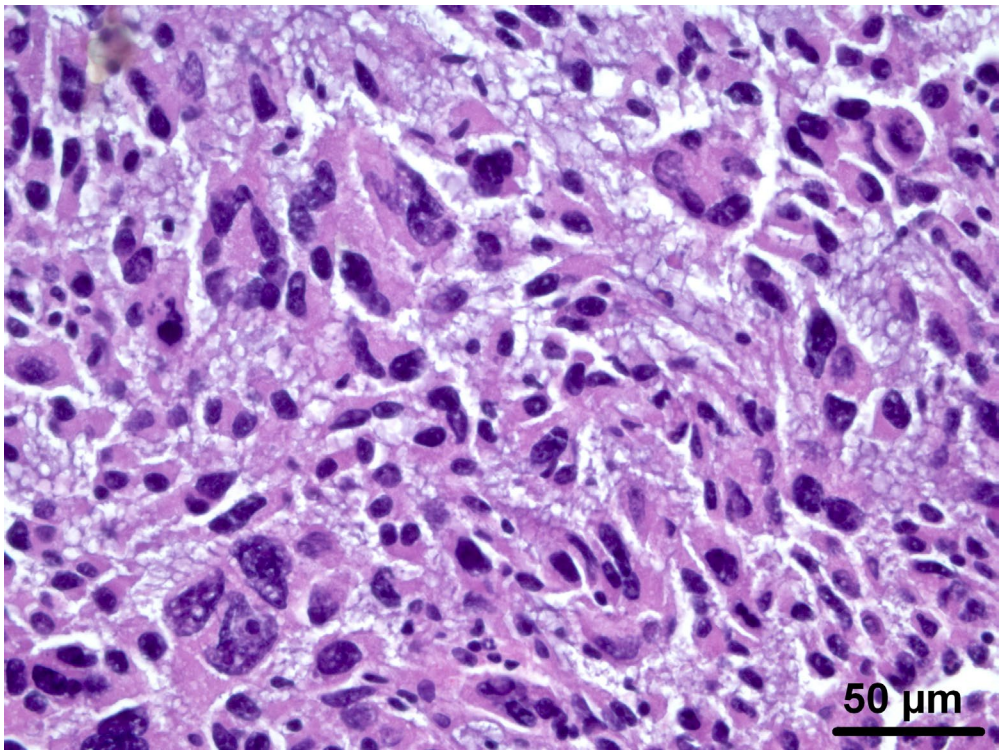

b)

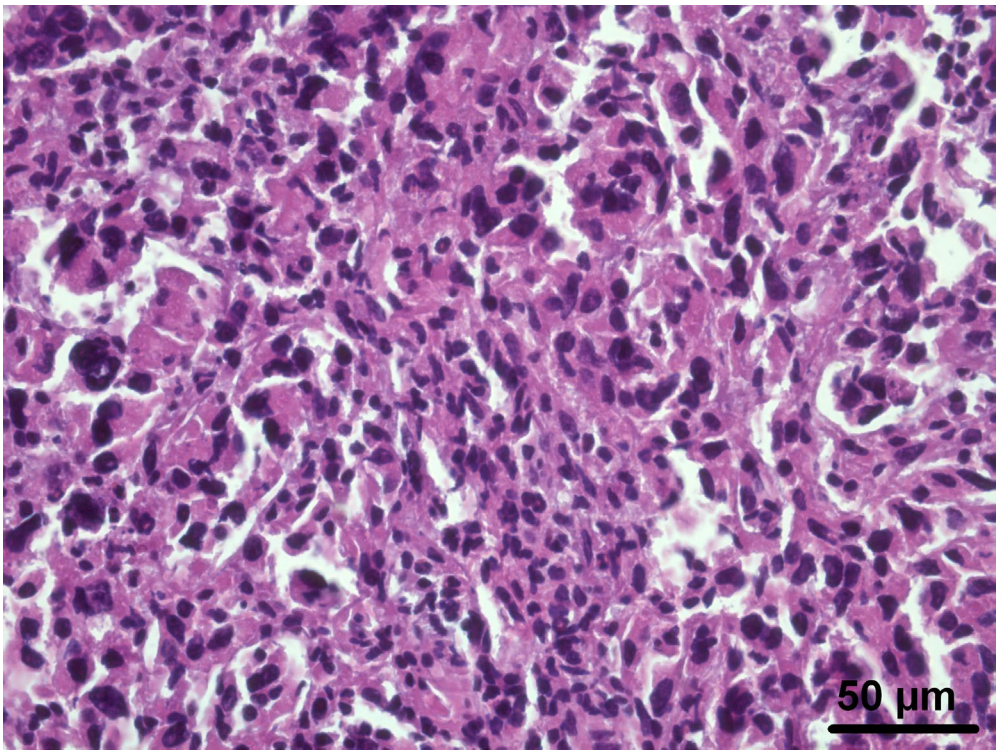

Figure legends

Figure 1. HRMAS spectral pattern of a N-FMW GL261 glioma tissue sample between 0.5 and 4.5 ppm, acquired at 37^{o} C with 512 transients and *pulse-and-acquire* sequence and the tentative assignments of the major resonances according to [11,42]. Mobile lipids (ML), lactate (Lac), alanine (Ala), acetate (Ac), N-acetil aspartate (NAA), aspartate (Asp), glutamate + glutamine (Glx), creatine (Cr), Choline-containing compounds (ChCCp), phosphatidylcholne (PtdCho), taurine (Tau), myo-inositol (mI) and glycine (Gly).

Figure 2. HRMAS spectra from GL261 mouse glioma samples with FMW irradiation (bottom) and a different one without FMW irradiation (top). Red (top) and blue (bottom) spectra correspond to the first acquisition (t = 34min) and black spectra correspond to the last acquisition (t = 374min). Stars label signals (the ppm position at the peak maxima is given) with statistically significant changes between the first and the last spectra in non-irradiated samples, detected during time-course experiments. Insert shows an expanded view of the 3.18-3.26 ppm region. No significant change took place in FMW-irradiated samples. Please note that top and bottom spectra originate from different tumours.

Figure 3. Time-course curves for resonances showing the most significant changes with incubation time displaying the average ± SD values measured in different samples (n=3). The square symbols correspond to samples with FMW irradiation, whereas diamond symbols correspond to samples without FMW irradiation. Plots refer to the percentage of change for the intensity of selected signals from HRMAS spectra from each starting time point for spectra. During the 34min short acquisition incubation time experiment only 3 of the acquired spectra, at 2, 16 and 34min, are shown for clarity.

Figure 4. Post-HRMAS 4μm histopathological slide of GL261 glioma tissue samples stained with haematoxylin-eosin (40X magnification) a) N-FMW irradiated sample, b) FMW irradiated sample. In both slides, the histopathological analysis could detect tumoral cells with characteristic abnormal morphology, although some artifact as pyknotic nuclei, condensed chromatin and shrunk cytoplasm are also present.